Electron-photon coincidence study of heavy-noble-gas excitation at small scattering angles

K. E. Martus,* S.-H. Zheng, and K. Becker
Department of Physics, City College of the City University of New York, New York 10031
(Received 7 February 1991)

The electron–polarized-photon coincidence technique has been used to study the finer details of the excitation of the first excited states of the heavy noble gases neon, argon, and krypton by electron impact in the regime of large impact parameters (small scattering angles and intermediate impact energies). Measurements with higher statistical accuracy of the P_1 coherence parameter in forward scattering for excitation of the $(^2P_{1/2})ns'[\frac{1}{2}]_1^0(\text{“}^1P_1\text{”})$ state in neon ($n=3$) and argon ($n=4$) are reported along with P_1 measurements for both the $(^2P_{1/2})5s'[\frac{1}{2}]_1^0(\text{“}^1P_1\text{”})$ state and the $(^2P_{3/2})5s'[\frac{3}{2}]_1^0(\text{“}^3P_1\text{”})$ state in krypton for incident electron energies from 30 to 100 eV. All measurements are consistent with a P_1 value of $+1$, which is indicative of the dominance of direct excitation via transfer of orbital angular momentum. No evidence was found that exchange excitation via spin transfer plays a role in forward scattering at these energies, in agreement with theoretical predictions. A series of systematic measurements of the two linear coherence parameters P_1 and P_2 was carried out for excitation of the “$^1P_1$” state in argon and the “$^3P_1$” state in krypton at 50-eV impact energy and electron-scattering angles up to 25°. A detailed comparison with the predictions of the distorted-wave Born approximation and the first-order many-body theory reveals a generally satisfactory agreement and indicates that the theories are capable of reproducing the general features of the measured parameters as a function of scattering angle. Two parameters characterizing the angular part of the collisionally induced P-state charge cloud, the alignment angle γ, and the linear polarization P_{lin}, were extracted from the measured P_1 and P_2 values. The agreement between experiment and theory in the case of γ is in general good, whereas it is somewhat poorer as far as P_{lin} is concerned. This indicates that the theoretical models are quite good in predicting the alignment angle of the collisionally induced charge cloud in the scattering plane, but less capable of predicting the exact shape of the charge cloud.

I. INTRODUCTION

Electron-photon angular- and polarization-correlation measurements have been carried out for more than 15 years to study inelastic electron-atom collisions at the most fundamental level where comparisons between experiment and theory can be made at the level of excitation amplitudes and their interference (coherence parameters) rather than at the level of moduli-squared excitation amplitudes (cross sections) [1–7]. Coincidence experiments detect the inelastically scattered electrons which have excited a particular target state in coincidence with the subsequently emitted decay photons either without regard for the light polarization (angular correlations) or after a linear and/or circular polarization analysis of the emitted radiation has been performed (polarization correlations). Much of the emphasis of the earlier work focused on the excitation of the $2\,^1P_1$ state in helium from the $1\,^1S_0$ ground state which has been the most thoroughly investigated excitation process both experimentally and theoretically. Subsequently, the focus shifted to studies of more complex target atoms, to studies of the excitation of states with higher orbital angular momentum quantum numbers, and to studies of excited triplet states. Several reviews have summarized the progress in the field at regular intervals [2,3,6,7]. We would like to mention in particular the review by Andersen, Gallagher, and Hertel [6] which not only provided the most comprehensive compilation of experimental and theoretical coincidence data prior to 1987, but these authors also introduced a set of frame-independent parameters, the natural parameters $(\gamma, L_\perp, P_{\text{lin}}, \rho_{00})$, which are by now generally accepted as the standard parameter set used to present the results of coherence measurements and calculations. The natural parameters are related directly to the shape and dynamics of the angular part of the collisionally induced excited-state charge cloud.

Recently, electron-photon coincidence studies of heavy targets such as the heavy noble gases and mercury have become the subject of intense activity. These atoms allow a detailed investigation of the role of the various spin effects (e.g., exchange, spin-orbit interactions) in the excitation process and facilitate a stringent test of how theoretical models incorporate relativistic effects for both the target electrons and the continuum electron. Coherence experiments which investigate the excitation of heavy atoms with unpolarized incident electrons and without performing a spin analysis of the scattered electrons require the measurement of four independent parameters in two different geometries for a complete mapping of the reduced density matrix of the excited state [8]. The elements of the reduced density matrix in this particular case are averaged over the spins of the incident electrons and summed of the spins of the scattered electrons.

The excitation of the heavy noble gases has emphasized primarily the excitation of the first excited states,

i.e., the excitation of the spin-orbit-coupled $(^2P_{1/2})ns'[\frac{1}{2}]_1^0(\text{“}\,^1P_1\text{”})$ and $(^2P_{3/2})ns[\frac{3}{2}]_1^0(\text{“}\,^3P_1\text{”})$ states ($n=3,4,5,6$ for Ne, Ar, Kr, and Xe). Both excited states are often pictured as linear combinations of LS-coupled singlet and triplet states (see, e.g., Andersen, Gallagher, and Hertel [6]). Experimentally determined coherence parameters for heavy-noble-gas excitation have been obtained by several groups using either the angular-correlation technique [9–15] or the polarization-correlation technique [5,16–22]. On the theoretical side, Balashov, Kozhevnikov, and Magunov [23] used an eight-state multichannel diffraction approximation (MCDA) to calculate the first coherence parameters in neon and argon, but their approach did not take spin-orbit effects into account. Bartschat and Madison [24] applied a distorted-wave Born approximation (DWBA) in a series of coherence-parameter calculations for all four heavy noble gases (neon, argon, krypton, and xenon). In addition, first-order many-body theory (FOMBT) calculations are available for Ne [25,26], Ar [27], and Kr [28,29]. In this paper we report a series of measurements of coherence parameters for the excitation of the$(^2P_{1/2})ns'[\frac{1}{2}]_1^0(\text{“}\,^1P_1\text{”})$ state in Ne, Ar, and Kr and of the $(^2P_{3/2})ns[\frac{3}{2}]_1^0(\text{“}\,^3P_1\text{”})$ state in Kr for intermediate impact energies and small electron-scattering angles (i.e., in the regime of large impact parameters). Specifically, measurements of the linear coherence parameter P_1 in forward scattering were carried out for Ne, Ar, and Kr for energies from 30 to 100 eV together with a series of measurements of P_1 and of the other linear coherence parameter P_2 in Ar and Kr at 50 eV for electron-scattering angles up to 25°. Special care was exercised to ensure that the influence of instrumental effects on the measured parameters such as finite volume effects [30–33] and the finite angular acceptance of the electron analyzer [34] and of physical effects such as the depolarization due to hyperfine interactions (in Kr) [22], was either negligible or that the results were properly corrected for these effects. This paper is organized as follows: Sec. II reviews the theoretical background and the history of previous experiments, Sec. III discusses the experimental details and the data analysis, the results are presented and discussed in Sec. IV, and Sec. V summarizes the conclusions that can be drawn from the present experiments.

II. THEORETICAL BACKGROUND AND HISTORY OF PREVIOUS WORK

Electron-photon angular- and polarization-correlation measurements are a well-established experimental technique in electron collision physics since the early 1970s. The groundwork for the theoretical description of these experiments has been laid by Rubin *et al.* [35], Wykes [36], Macek and Jaecks [37], and Fano and Macek [38]. For a detailed discussion, the reader is referred to these articles or to one of the excellent reviews on the subject by Blum and Kleinpoppen [2], Slevin [3], Andersen, Gallagher, and Hertel [6], and Slevin and Chwirot [7]. The review by Andersen, Gallagher, and Hertel [6] not only provides the most comprehensive compilation of coherence data prior to 1987, but it also discusses the various parameter sets that have been used to express the results of coincidence and coherence studies and introduces a frame-independent parametrization scheme, the natural parameters $(\gamma, L_\perp, P_{\rm lin}, \rho_{00})$.

In the excitation of the heavy noble gases by electron impact, an upper state with total angular momentum $J_1=1$ and odd parity is excited from the even parity ground state with $J_0=0$. Unpolarized incident electrons are used and no spin analysis of the scattered electrons is performed. The reduced density matrix [8] describing the excited state in this case is characterized by five independent parameters, one cross section, and four coherence parameters. The natural parameters of Andersen, Gallagher, and Hertel [6] which are related to the shape and dynamics of the angular part of the collisionally induced excited-state charge cloud are defined as follows: γ, the alignment angle of the excited-state charge cloud relative to the incident electron beam axis, $P_{\rm lin}^+$, the linear polarization in the scattering plane, $L_\perp^+$, the orbital angular momentum perpendicular to the scattering plane that is transferred to the atom in the collision, and ρ_{00}, the relative height of the charge cloud perpendicular to the scattering plane at the point of origin. The "+" superscript indicates positive reflection symmetry with respect to the scattering plane [5,6]. In coherence experiments, one typically measures two linear (P_1, P_2) and one circular (P_3) polarization-correlation parameter perpendicular to the scattering plane, and one additional linear polarization-correlation parameter, P_4, is measured in the scattering plane. Each parameter is the result of two intensity measurements for different orientations of the polarization analyzer:

$$P_1=[I(0°)-I(90°)]/[I(0°)+I(90°)]\beta^{-1}\,, \tag{1a}$$

$$P_2=[I(45°)-I(135°)]/[I(45°)+I(135°)]\beta^{-1}\,, \tag{1b}$$

$$P_3=(I^+-I^-)/(I^++I^-)\beta^{-1}\,, \tag{1c}$$

$$P_4=[I(0°)-I(90°)]/[I(0°)+I(90°)]\beta^{-1}\,. \tag{1d}$$

Here $I(\alpha)$ denotes the photon intensity measured for a polarizer orientation α with respect to the electron beam axis, I^+ and I^- refer to right- and left-handed circularly polarized light, and β denotes the polarization sensitivity of the polarization analyzer which can be significantly smaller than unity for reflection-type devices which have to be used in the vacuum ultraviolet region (VUV) (cf. Sec. III C). The relationship between the experimentally determined parameters (1a)–(1d) and the previously defined natural parameters is given by

$$\gamma=\tfrac{1}{2}\arctan(P_2/P_1)\,, \tag{2a}$$

$$P_{\rm lin}^+=[(P_1)^2+(P_2)^2]^{1/2}\,, \tag{2b}$$

$$L_\perp^+=(-P_3) \tag{2c}$$

for the "+" part,

$$L_\perp=(1-\rho_{00})(-P_3) \tag{2c'}$$

for the full P state, and

$$\rho_{00}=[(1+P_1)(1-P_4)]/[4-(1-P_1)(1-P_4)]\,. \tag{2d}$$

The total polarization P_{tot} which is defined as

$$P_{\text{tot}}^{+}=[(P_{\text{lin}}^{+})^2+(L_{\perp}^{+})^2]^{1/2}$$
$$=[(P_1)^2+(P_2)^2+(P_3)^2]^{1/2} \quad (2e)$$

is a measure for the degree of coherence in the excitation process. We note that the quantity P_{lin}^{+} is frame independent and thus provides a more satisfactory description [6] than the often used parameter $|\mu_c|$, the level of coherence as introduced by Blum and Kleinpoppen [2]. In the absence of depolarizing effects due to, e.g., hyperfine interactions, a value of $P_{\text{tot}}^{+}=+1$ for the emitted radiation indicates total coherence of the excitation process.

In comparison to the excitation of helium or hydrogen which have been described by a variety of theoretical models, both perturbative and *ab initio,* the theoretical situation in the heavy noble gases is limited to only a few calculations. Aside from the MCDA calculations of Balashov, Kozhevnikov, and Magunov [23] for neon and argon, which did not include spin-orbit effects, the most comprehensive theoretical calculations of coherence parameters for heavy-noble-gas excitation are those using the DWBA [24] and the FOMBT [25–29]. Both theories are first-order, perturbative theories which are expected to be valid for impact energies above about 2–3 times the threshold energy or above about 30 eV for the heavy noble gases. Experimental determinations of coherence parameters for heavy-noble-gas excitation have also been scarce. In addition, they have often carried large error margins. Moreover, it has been demonstrated recently that some of the experimental data measured before about 1988 were seriously affected by instrumental effects such as the finite acceptance angles of detectors [19,34] and/or the finite dimension of the interaction volume [30–33]. In the absence of a large body of reliable experimental data which could have stimulated a more detailed comparison between experiment and theory, there had been little pressing need to develop theoretical models for heavy-noble-gas excitation which are more sophisticated than the available first-order perturbative theories. Several major experimental breakthroughs occurred during the last two years. Martus, Becker, and Madison [34] and Martus and Becker [19] demonstrated the need to account for the finite angular acceptance of the electron analyzer when interpreting measured coherence parameters in order to preclude erroneous conclusions about the role of spin effects. Zetner *et al.* [30,31] were able to show that the "mysterious" asymmetry in the superelastic scattering experiment of Register *et al.* [39] could be explained in terms of an experimental artifact, viz., the finite size of the interaction volume. They also demonstrated that both out-of-plane angular-correlation measurements and in-plane polarization-correlation measurements can be prone to similar instrumental effects. Independently, Simon *et al.* [32] and van der Burgt, Corr, and McConkey [33] corroborated the findings of Zetner *et al.* [30,31] and showed that small angle measurements of the coherence parameter P_4 in mercury and in the heavy noble gases are particularly strongly influenced by the finite size of the interaction volume and the alignment of the electron beam. Their findings clarified ambiguities that had arisen from previously reported data which had indicated a significant probability for spin-flip processes in inelastic electron collisions with heavy noble gases and mercury in a regime where neither theory nor physical intuition rendered such spin effects probable. Khakoo and McConkey [5] and Corr *et al.* [21,22] verified that $P_{\text{tot}}^{+}=+1$ holds for the excitation of Ne and Ar in the regime of small scattering angles and similarly for Kr and Xe provided the depolarization caused by hyperfine interactions is taken into account properly for these two atoms. Both natural Kr and Xe contain isotopes with a nuclear spin different from zero.

These conclusions drawn from the currently available data on heavy-noble-gas excitation in the regime of large impact parameters are supported by both the DWBA and the FOMBT calculations which predict a negligible probability for spin flip ($\rho_{00}=0$) and essentially total coherence in the excitation process ($P_{\text{tot}}^{+}=+1$) in that scattering regime. This, in turn, allows further experimental studies in that regime to focus primarily on the measurement of two of the three coherence parameters P_1, P_2, and P_3. The linear parameters P_1 and P_2 are more readily accessible to a measurement. For a complete characterization, $(P_3)^2$ can be obtained from Eq. (2e), which determines P_3 or $L_{\perp}^{+}$ except for the sign. The fourth parameter ρ_{00} which can be extracted from P_1 and P_4 is essentially zero. This paper reports new results of experimental determinations of the coherence parameters for the excitation of the heavy noble gases at large impact parameters. Firstly, we report measurements of the P_1 parameter in forward scattering for the "$^1P_1$" state in Ne and Ar with improved statistical accuracy compared to our previous results [19] along with new data for the "$^1P_1$" state and the "$^3P_1$" state in Kr. We also report measurements of the P_1 and P_2 parameters for "$^3P_1$" excitation in Kr and "$^1P_1$" excitation in Ar at 50 eV and electron-scattering angles up to 25°. A detailed comparison is made with the predictions of both DWBA and FOMBT calculations and, where possible, also with the experimental results reported by other authors. Special care was exercised to incorporate into the quoted uncertainties statistical uncertainties as well as all possible sources of systematic uncertainties to enable a meaningful and critical comparison between experiment and theory.

III. DESCRIPTION OF THE EXPERIMENTAL APPARATUS

A brief description of the electron–polarized-photon coincidence apparatus employed in the present studies has been given in previous publications from this laboratory where initial results of this work have also been presented [19,20]. A block diagram of the essential components of the experiment is shown in Fig. 1.

A. General description

The apparatus is housed in a stainless-steel vacuum chamber which is routinely pumped down to a base pressure in the 10^{-8}-Torr range by a Sargent Welch model

3133 turbomolecular pump backed by a model 8851 direct-drive roughing pump. The residual magnetic field inside the vacuum chamber is reduced to less than 10 mG by a single layer of magnetic shielding. In addition, the monochromator and analyzer sections of the electron spectrometer are mounted in two separate, magnetically shielded boxes to reduce the magnetic fields along the path of the electron beam even further. The apparatus is continuously kept at a slightly elevated temperature to improve the long-term stability of the performance of the electron spectrometer and to prevent the deterioration of the gold surfaces of the reflection-type polarization analyzers.

The target gas beam is introduced by effusing neon, argon, krypton, or helium gas (research grade purity from Air Products and Chemicals Inc.) through a single stainless-steel hypodermic needle of 0.3 mm inner diameter and 5 mm length. The driving pressure in the gas line is continuously monitored by a MKS Baratron gauge. The gas load is kept as low as possible to prevent radiation trapping. The measured polarization-correlation parameters were found to be independent of the driving pressure as long as the background pressure in the vacuum chamber did not exceed 5×10^{-7} Torr as determined from the reading of a conventional Bayard-Alpert ionization gauge which was appropriately corrected for the different ionization potentials of the various target gases [40].

B. The electron beam

The electron spectrometer used in this experiment incorporates two commercially available double-focusing electrostatic analyzers (Comstock model AC 901), one for the production of an energy selected incident beam, and one for the analysis of the inelastically scattered electrons. Various modifications of the commercially available instrument were incorporated into the design of our spectrometer to improve its overall performance and to achieve a better control over the angular acceptance of the analyzer section. A small hole in the back of the monochromator collinear with the axis of the monochromator output optics and a slightly larger hole in the back of the analyzer allow the mechanical alignment of the electron spectrometer with a laser beam. A collector plate mounted behind the hole in the back of the analyzer served as a Faraday cup and allowed us to monitor the unscattered, straight-through electron beam when the analyzer was positioned in the forward scattering direction, $\Theta_e=0°$. In addition, the current measured on this collector plate as a function of the scattering angle when the analyzer was rotated through the forward direction served as a measure of the full-width-at-half-maximum (FWHM) angular acceptance of the analyzer. Figure 2 shows the result of two such measurements for different entrance aperture sizes corresponding to a FWHM acceptance angle of 4° and 2.5°, respectively. Furthermore,

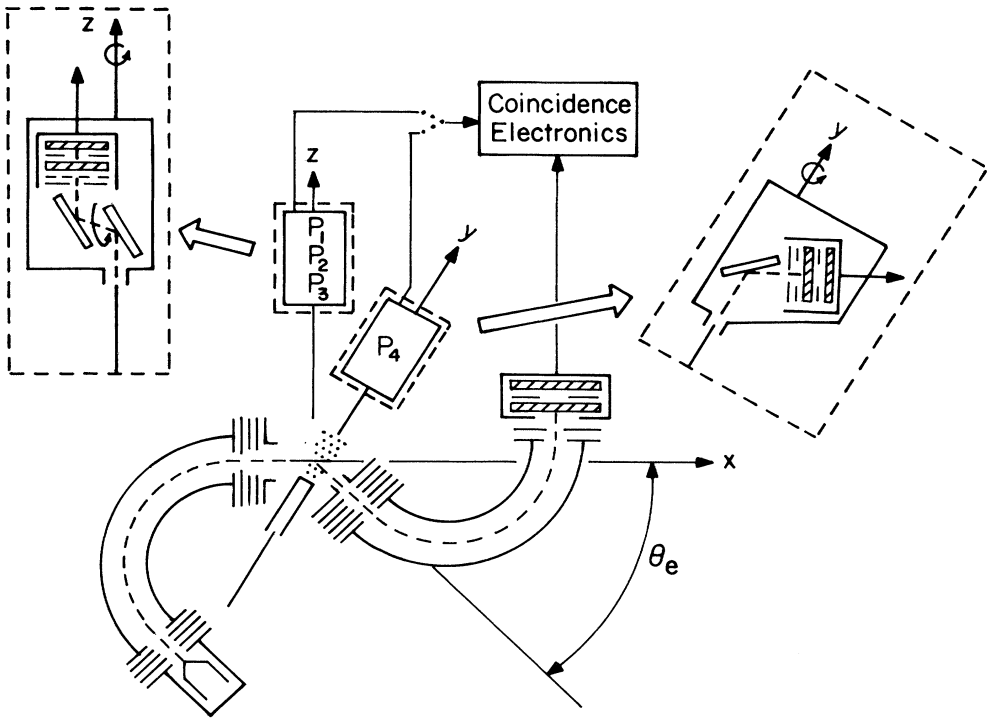

FIG. 1. Schematic diagram of the electron–polarized-photon coincidence apparatus. The box labeled P_1, P_2, P_3 represents the polarization analyzer for linear or circular polarization analysis of impact radiation emitted perpendicular to the scattering plane and the box labeled P_4 represents a polarization analyzer for linear polarization analysis in the scattering plane.

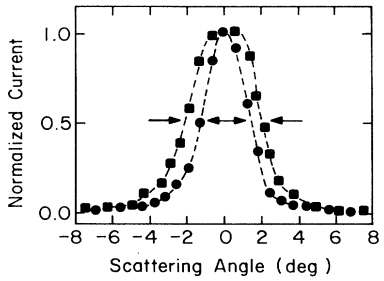

FIG. 2. Normalized current measured in a Faraday cup mounted in the back of the electron analyzer as a function of electron-scattering angle (see text for details). The two data sets were obtained for different entrance aperture sizes and correspond to FWHM angular acceptance angles of the analyzer of 2.5° (full circles) and 4° (full squares) as indicated by the arrows.

this current measurement was one of three independent *in situ* determinations of the forward scattering direction. The other two methods utilize (1) the symmetry of the inelastic scattering signal about $\Theta_e=0°$ and (2) a measurement of the P_2 coherence parameter for scattering angles symmetric about $\Theta_e=0°$, e.g., for $\Theta_e=\pm 5°$, since the P_2 parameter goes through zero at $\Theta_e=0°$ with a steep gradient. A combination of the three independent methods allowed us to determine the forward scattering direction to within $\pm 0.5°$. Once the forward direction was established, all electron-scattering angles were referenced to this direction. The unavoidable mechanical backlash in the rotary motion feedthrough that is used to rotate the electron analyzer limits the accuracy in the determination of the nonzero electron scattering to approximately $\pm 1.5°$.

The monochromator produces a spatially and energetically well-defined electron beam of variable energy from 10 to 120 eV. Incident beam currents ranging from 5 to 300 nA could be obtained depending on the impact energy and the desired energy resolution. The inelastically scattered electrons were collected by a similar analyzer, energy selected, and detected by either a dual channel-plate detector or a channel electron multiplier. Typical count rates in the electron channel ranged from 1 to 25 kHz. For measurements in the forward direction, beam currents of 20 nA or less were used in order to limit the intensity of the unscattered, straight-through beam that entered the analyzer and that can lead to an unwanted background in the energy loss spectrum. The overall energy resolution of the electron spectrometer was determined from the FWHM of the energy loss peak of the "$^3P_1$" state in Kr and ranged from 150 to 400 meV. The beam energy was calibrated relative to the excitation function of the ultraviolet-emitting levels of Ne as reported in the work of Brunt, King, and Read [41]. The pronounced resonance structure in their spectrum labeled as b_4 at 17.05 eV served as a reference point. Contact potentials were found to be in the range of a few tenths of a volt and were stable to within ± 0.2 V over periods of several weeks.

C. The polarization analyzer

The resonance emissions of the rare gases are in the vacuum ultraviolet region of the optical spectrum at, respectively, 73.6/74.4 nm (Ne), 104.8/106/7 nm (Ar), and 116.5/123.6 nm (Kr). Linear and circular polarization analysis of vuv radiation requires the use of reflection rather than transmission optics. Our experiment employs either a single-reflection polarization analyzer or a double-reflection device similar to the one described by Westerveld *et al.* [42]. Since the focus of the present investigations was on the linear parameters P_1 and P_2, the vast majority of data was obtained with a single-reflection polarization analyzer in an effort to increase the photon count rate. The polarization analyzers employ gold coated optical flats with a flatness of $\lambda/10$ at 100 nm as reflecting surfaces. Gold was chosen on the basis of the wavelength dependence of its optical constants which ensures an essentially constant polarization efficiency and a $90\pm 2°$ phase difference between the parallel and perpendicular components of the reflected light for a fixed angle of incidence (58.5°, cf. below) over a wide wavelength range from 50 to 130 nm [41]. In addition, gold surfaces in a high vacuum environment are very stable over time, in particular when kept at a slightly elevated temperature. All reflectors were oriented at an angle of incidence of 58.5°. This angle of incidence results in a nominal linear polarization sensitivity around 0.66 ± 0.04 for a single reflection over the entire wavelength range 50–125 nm [43]. The actual polarization sensitivity of our analyzer was typically somewhat lower (cf. discussion below). The vuv photons were detected by a CsI coated channel electron multiplier. Typical count rates in the photon channel ranged from 150 to 800 Hz.

The polarization sensitivity of the polarization analyzers was determined *in situ* and checked regularly. The initial determination of the polarization efficiency (and of the alignment of the polarization analyzer relative to the position of the interaction region) was performed by mapping out the complete 0–360° noncoincident radiation pattern of the He vuv resonance emissions perpendicular to the scattering plane in steps of 15° following 50-eV electron impact on He. The positioning of the polarization analyzers relative to the scattering plane and the interaction region was deemed acceptable when the radiation pattern was symmetric to within 2%, i.e., when the measured (normalized) intensities $I(\alpha)$ and $I(\alpha+\pi)$ were found to agree to within 2%, where α denotes the orientation of the polarization analyzer relative to the direction of the incident electron beam. The effect of the finite acceptance of the polarization analyzer on the polarization efficiency has been investigated by Khakoo and McConkey [5]. In our case, this correction is negligible. The polarization efficiency was determined by comparing the ratio R defined as

$$R=[I(0°)+I(180°)]/[I(90°)+I(270°)]$$

extracted from the 50-eV noncoincident He radiation pattern with the most recently measured [44] and calculated [45] value for the linear polarization (0.52 ± 0.02). We found values of the polarization sensitivity of typical-

ly 0.59±0.03, which is somewhat lower than the maximum sensitivity determined from the optical constants of gold (see discussion above). This is most likely caused by surface imperfections and/or by a slight degradation of the gold surface. The polarization efficiency as determined from the He radiation pattern was subsequently used to determine the P_1 coherence pattern in forward scattering for excitation of the "$^1P_1$" state in Ne, Ar, and Kr at 50 eV. Once it had been established that P_1 was unity to within 3% for these cases [19], subsequent determinations of the polarization efficiency were always referenced to the measured P_1 coherence parameter at 50 eV and $\Theta_e=0°$.

D. Data acquisition and analysis

The signals from the electron and photon detectors were processed by standard coincidence circuitry (fast charge sensitive preamplifier, constant fraction discriminator, delay line amplifier, and single channel analyzer) and fed into a time-to-amplitude converter (TAC). The TAC output was stored in a Tracor Northern model 1710 multichannel analyzer operated in the pulse height analysis mode. Each polarization-correlation parameter was determined from coincident intensities measured at two different orientations, $I(\alpha)$ and $I(\alpha+\pi/2)$, of the polarization analyzer. In our experiments, the polarization analyzer was rotated every 200 or 500 s between the two positions to average out long-term drifts and variations in the electron beam current and gas beam density. The two signals were stored in separate halves of the MCA memory and subsequently transferred to a Macintosh II laboratory computer for further data analysis. In many cases, two independent measurements were carried out to obtain one coherence parameter. One measurement for the polarization analyzer rotating between α and $\alpha+\pi/2$ and another measurement for angles $\alpha+\pi$ and $\alpha+3\pi/2$. Only data are reported for which the two measurements agreed to within half of their combined error bars. Error bars reported here include all systematic uncertainties and one standard deviation of counting statistics.

IV. RESULTS AND DISCUSSION

The spin-orbit-coupled $ns'[\frac{1}{2}]_{J=1}$ and $ns[\frac{3}{2}]_{J=1}$ excited states of the heavy noble gases are often described as linear combinations of Russel-Saunders coupled singlet and triplet states [6]. Measurements reported in this paper were carried out for the excitation of those states that are of predominantly singlet character, i.e., the $(^2P_1/2)ns'[\frac{1}{2}]_1^0$("$^1P_1$") state of Ne ($n=3$) and Ar ($n=4$) and the $(^2P_{3/2})5s[\frac{3}{2}]_1^0$("$^3P_1$") state of Kr. We note that the distinction between the "$^3P_1$" state and the $(^2P_{1/2})5s'[\frac{1}{2}]_1^0$("$^1P_1$") state of Kr is somewhat meaningless, since the singlet-triplet mixing coefficients for both states are almost equal [6] with a slight dominance of the singlet component in the "$^3P_1$" state and a slight dominance of the triplet component in the "$^1P_1$" state. The theoretical predictions for the coherence parameters are very similar for both Kr states at large impact parameters. While most measurements in Kr focused on the excitation of the singlet-dominated "$^3P_1$" state, some measurements of the excitation of the triplet-dominated "$^1P_1$" state were carried out to verify this prediction. In addition, the P_1 measurements in forward scattering were carried out for both excited Kr states.

A. Measurements in forward scattering

A measurement of the P_1 coherence parameter in forward scattering reveals information about the relative contributions of direct excitation via transfer of orbital angular momentum versus exchange excitation via spin transfer without having to use spin polarized incident electrons and without having to analyze the spin polarization of the scattered electrons [46,47]. Inspection of the angular momentum selection rules appropriate to this geometry shows that a P_1 value of $+1$ indicates the presence of pure orbital angular momentum transfer, i.e., only direct excitation of the *LS*-coupled singlet component of the excited state occurs. Conversely, a value $P_1=-1$ is the signature of pure exchange excitation of the *LS*-coupled triplet component, i.e., pure spin angular momentum transfer. A P_1 value between $+1$ and -1 reveals the relative contributions of the two excitation mechanisms. Theoretical calculations [24–29] predict a P_1 value of essentially $+1$ in forward scattering for both excited states in all four heavy noble gases at all but the very lowest impact energies. These predictions were verified experimentally for Ne and Ar in an earlier publication from this laboratory [19] which clarified a previous discrepancy between theory and experiment [16]. Figure 3 summarizes the results of our most recent measurements of the P_1 coherence parameter in forward scattering ($\Theta_e=0\pm0.5°$) for excitation of the $ns'[\frac{1}{2}]_1^0$ state in Ne ($n=3$), Ar ($n=4$), and Kr ($n=5$) and of the $5s[\frac{3}{2}]_1^0$ state in Kr for impact energies from 30 to 100 eV. For clarity of presentation, only the nominal P_1 values corrected for all instrumental effects (for details, see Refs. [19] and [34]) are shown in Fig. 3. The statistical accuracy of the Ne data and, in particular, of the Ar data has been improved significantly compared to the previously reported results [19]. The P_1 data for excitation of the two states in Kr in forward scattering [Figs. 3(c) and 3(d)] are consistent with the theoretical prediction of $P_1=+1$ and corroborate the experimental findings in Ne and Ar. All nominal P_1 values obtained in the course of this work are summarized in Table I. The measurements unequivocally demonstrate that the excitation of the heavy noble gases in forward scattering at intermediate energies is dominated by the direct excitation of the *LS*-coupled singlet component (i.e., by orbital angular momentum transfer) and that spin transfer plays essentially no role.

B. Measurements at small electron-scattering angles

In general, all four independent coherence parameters as introduced in Eqs. (1a)–(1d) are required for a complete characterization of the excitation process away from the forward direction. In the regime of small

scattering angles and intermediate impact energies (i.e., at large impact parameters), it can be argued, however, that the two linear coherence parameters P_1 and P_2 carry the most significant information about the excitation process. Corr *et al.* [21] have recently verified that spin-flip processes play essentially no role in heavy-noble-gas excitation in the regime of small electron-scattering angles up to about 50°. Their experiments revealed P_4 values of essentially unity in that regime which implies that the fourth coherence parameter, ρ_{00}, is zero [cf. Eq. (2d)]. These experimental findings have been corroborated by theoretical predictions. Furthermore, a total polarization of $P_{\rm tot}^{+}=+1$ implying full coherence of the excitation process has been observed experimentally for heavy-noble-gas excitation at small scattering angles in agreement with theoretical predictions. This allows extraction of the third coherence parameter, e.g., P_3 (or more precisely $|P_3|$) from a measurement of the other two parameters P_1 and P_2. It should be noted that the observation of full coherence in Kr and Xe was only verified [21] after proper allowance had been made for hyperfine depolarization caused by the existence of krypton and xenon isotopes with nonzero nuclear spin in natural Kr and Xe.

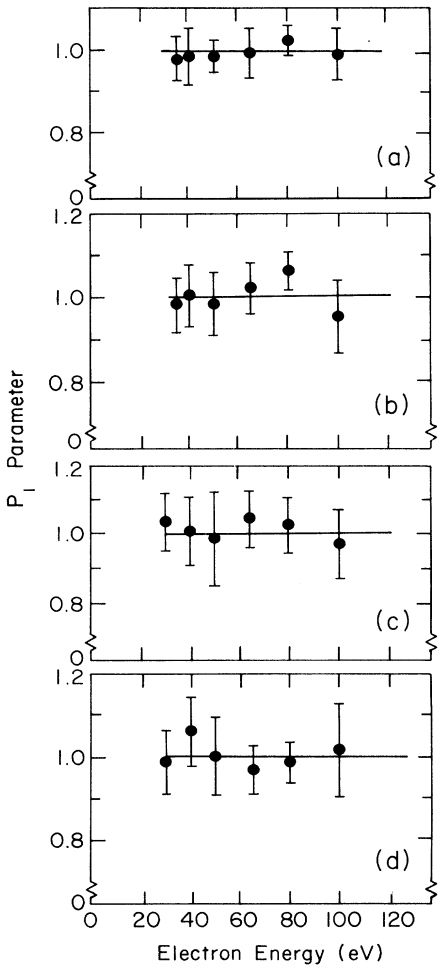

FIG. 3. P_1 coherence parameter in forward scattering as a function of impact energy for excitation of the $(^2P_{1/2})3s'[\frac{1}{2}]_{J=1}$ state in Ne (a), the $(^2P_{1/2})4s'[\frac{1}{2}]_{J=1}$ state in Ar (b), the $(^2P_{1/2})5s'[\frac{1}{2}]_{J=1}$ state in Kr (c), and the $(^2P_{3/2})5s[\frac{3}{2}]_{J=1}$ state in Kr (d). The data points have been corrected for all instrumental effects (see text for details). Error bars include all systematic uncertainties and one standard deviation of counting statistics. The solid lines ($P_1=+1$) in each figure indicate the theoretical prediction of both the DWBA [24] and the FOMBT [25–29].

We chose to measure the two linear coherence parameters P_1 and P_2 at 50-eV impact energy for excitation of the $(^2P_{1/2})4s'[\frac{1}{2}]_{J=1}$ state in Ar and the $(^2P_{3/2})5s[\frac{3}{2}]_{J=1}$ state in Kr for electron-scattering angles from 0° to 25°. The preference for carrying out the measurement of a linear coherence parameter (P_1 or P_2) compared to a measurement of the circular coherence parameter P_3 is the result of the fact that linear coherence parameter measurements can be performed with higher statistical accuracy (i.e., a higher signal-to-background ratio) and with a reduced systematic uncertainty. Furthermore, these measurements are significantly less time consuming, since a measurement of P_3 requires either the previous measurement of both P_1 and P_2 at the same impact energy and electron-scattering angle or the measurement of four independent coincident intensities as discussed by Westerveld *et al.* [42] and Khakoo and McConkey [5].

TABLE I. Coherence parameter P_1 in forward scattering for various targets and impact energies. Given are the nominal P_1 values corrected for all instrumental effects (see Refs. [19] and [34] for details). The quoted errors include all systematic uncertainties and one standard deviation of counting statistics.

Gas	State	Energy (eV)	Nominal P_1 value
Ne	$3s'[\frac{1}{2}]_1^0$	35	0.98±0.05
Ne	$3s'[\frac{1}{2}]_1^0$	40	0.99±0.07
Ne	$3s'[\frac{1}{2}]_1^0$	50	0.99±0.04
Ne	$3s'[\frac{1}{2}]_1^0$	65	1.00±0.06
Ne	$3s'[\frac{1}{2}]_1^0$	80	1.02±0.03
Ne	$3s'[\frac{1}{2}]_1^0$	100	0.99±0.06
Ar	$4s'[\frac{1}{2}]_1^0$	35	0.99±0.07
Ar	$4s'[\frac{1}{2}]_1^0$	40	1.01±0.07
Ar	$4s'[\frac{1}{2}]_1^0$	50	0.98±0.07
Ar	$4s'[\frac{1}{2}]_1^0$	65	1.02±0.06
Ar	$4s'[\frac{1}{2}]_1^0$	80	1.07±0.04
Ar	$4s'[\frac{1}{2}]_1^0$	100	0.95±0.08
Kr	$5s[\frac{3}{2}]_1^0$	30	1.05±0.08
Kr	$5s'[\frac{1}{2}]_1^0$	30	0.99±0.08
Kr	$5s[\frac{3}{2}]_1^0$	40	1.01±0.10
Kr	$5s'[\frac{1}{2}]_1^0$	40	1.06±0.09
Kr	$5s[\frac{3}{2}]_1^0$	50	0.98±0.14
Kr	$5s'[\frac{1}{2}]_1^0$	50	1.00±0.11
Kr	$5s[\frac{3}{2}]_1^0$	65	1.05±0.09
Kr	$5s'[\frac{1}{2}]_1^0$	65	0.96±0.08
Kr	$5s[\frac{3}{2}]_1^0$	80	1.03±0.09
Kr	$5s'[\frac{1}{2}]_1^0$	80	0.98±0.07
Kr	$5s[\frac{3}{2}]_1^0$	100	0.97±0.10
Kr	$5s'[\frac{1}{2}]_1^0$	100	1.02±0.14

1. Measurements of the P_1 and P_2 coherence parameters

The measured P_1 and P_2 parameters for excitation of the $4s'[\frac{1}{2}]_1^0$ state of Ar at 50-eV impact energy and electron-scattering angles up to 25° are shown in Fig. 4. The experimental data are compared with the results of the DWBA calculations of Bartschat and Madison [24] (full line) and the FOMBT calculations of de Paixao, Padial, and Csanak [27] (dashed line). Also shown is the result of a first Born approximation, FBA (—·—·—·). The experimental error bars incorporate all systematic uncertainties and one standard deviation of counting statistics. Where no error bars are shown, the combined uncertainty is smaller than the plot symbol. All three theories predict a rapid decline of both P_1 and P_2 in the scattering regime between 0° and 15°. Both the DWBA and the FOMBT predict a pronounced minimum in P_1 and P_2 followed by a steep increase at scattering angles around 30°. The FBA, on the other hand, starts to deviate drastically from the other two theories around 10–15°. The measured data follow the general trend predicted by the DWBA and the FOMBT quite closely. This means that the FBA breaks down at comparatively large impact parameters (or small scattering angles). The differences between the theoretical predictions of the DWBA and the FOMBT are generally small in the scattering regime under study, which makes it difficult to determine which theory provides a better description of the measured data. The P_2 data seem to be slightly more consistent with the results of the FOMBT. It should also be noted that the rapid variations in P_1 and P_2 as a function of scattering angle are difficult to measure accurately in view of (1) the finite angular resolution of the electrostatic energy analyzer (2.5–4° FWHM) and (2) the finite precision in the determination of the nominal scattering angle (±1.5°) in our experiment. With that in mind, the agreement between experiment and theory has to be considered quite good. We note that the finite angular resolution and the accuracy in the determination of the scattering angle reported in this work are typical for this kind of experiment, even though their potential influence on the measured data has not always been fully recognized. The first-order, perturbative theories, DWBA and FOMBT, appear to yield quantitatively satisfactory results. Furthermore, the fairly similar predictions of the DWBA and the FOMBT might indicate that the exact choice of the distorting potential is perhaps not very crucial in the regime of large impact parameters. All experimentally determined coherence parameters are listed in Table II together with values of the alignment angle and the linear polarization of the angular part of the collisionally induced charge cloud which can be extracted from P_1 and P_2 and which will be discussed later. Although there are no other experimental data available at 50-eV impact energy, measurements in Ar by Khakoo and

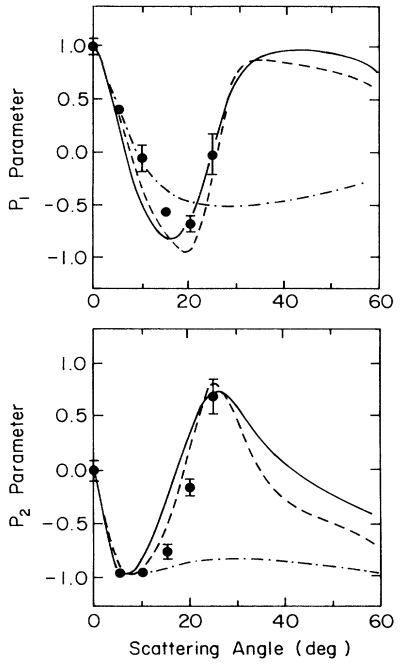

FIG. 4. P_1 and P_2 coherence parameter for excitation of the $(^2P_{1/2})4s'[\frac{1}{2}]_{J=1}$ state in Ar at 50 eV as a function of scattering angle. The three theoretical curves represent the predictions of the DWBA [24] (full line), the FOMBT [27] (dashed line) and a first Born approximation (—·—·—·). Error bars include all systematic uncertainties and one standard deviation of counting statistics. Where no error bar is indicated, the uncertainty is smaller than the plot symbol.

TABLE II. Coherence parameters P_1 and P_2 for excitation of the $4s'[\frac{1}{2}]_1^0$ state in Ar at an impact energy of 50 eV and various electron-scattering angles. Given are the nominal values of P_1 and P_2 corrected for all instrumental effects where necessary (see Refs. [19] and [34] for details) along with the extracted values for the alignment angle γ and the linear polarization P_{lin}. The quoted errors in P_1 and P_2 include all systematic uncertainties and one standard deviation of counting statistics.

Scattering angle (deg)	P_1	P_2	Alignment angle γ (deg)	Linear polarization P_{lin}
0±0.5	+0.98±0.07	−0.06±0.08	−1.8±2.4	0.98±0.09
5±1.5	+0.40±0.04	−0.98±0.06	−33.9±1.7	1.06±0.07
10±1.5	−0.11±0.12	−0.96±0.06	−48.3±3.7	0.97±0.13
15±1.5	−0.57±0.05	−0.78±0.07	−63.1±2.4	0.97±0.08
20±1.5	−0.67±0.06	−0.17±0.07	−82.9±6.1	0.69±0.08
25±1.5	−0.04±0.20	+0.67±0.20	+43.3±17.7	0.67±0.22

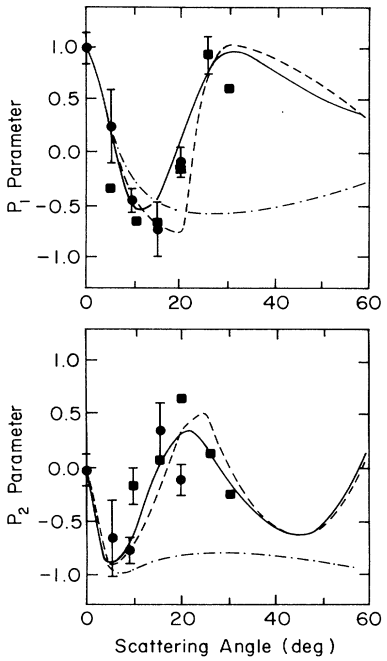

FIG. 5. Same as Fig. 4 for excitation of the $(^2P_{3/2})5s[\frac{3}{2}]_{J=1}$ state in Kr. Also shown are P_1 and P_2 values extracted from the angular-correlation measurements of Danjo *et al.* (full squares) [13]. Only one typical error bar is shown for their data which represents statistical uncertainty only. The P_2 data point extracted from their data at 5° is outside the meaningful range of P_2 values from -1 to $+1$ and is therefore not shown.

McConkey [5] carried out at 60 eV revealed very similar findings.

Figure 5 shows the measured P_1 and P_2 parameters for excitation of the $5s[\frac{3}{2}]_1^0$ state in Kr at 50 eV and scattering angles between 0° and 20° (full circles). Our data are again compared with the theoretical predictions of the DWBA [24], the FOMBT [29], and a FBA as well as with P_1 and P_2 values extracted from the angular-correlation measurements of Danjo *et al.* [13] (full squares). Our measured data are also listed in Table III. The general trend in both the calculations and the experimental data, viz., the pronounced minimum in both P_1 and P_2 at very small scattering angles, is very similar to that observed in Ar. In comparison, the prominent structures appear to be shifted slightly to smaller scattering angles and the FBA seems to break down at scattering angles even below 10°. The agreement between the experimental data and theoretical predictions of the DWBA and the FOMBT is satisfactory as was the case for Ar. In general, the agreement is quite good for the P_1 parameter, but less satisfactory for P_2, especially around 20°. The comparison between our polarization-correlation data and the angular-correlation data of Danjo *et al.* [13] is generally satisfactory for the P_1 values, but there are significant discrepancies in the case of the two measured P_2 data sets. No P_2 value at 5° extracted from the angular-correlation data of Danjo *et al.* [13] is shown, since the extracted P_2 value of -1.67 lies outside the range of physically meaningful P_2 values which have to be confined to the interval $+1$ to -1. Error bars for the angular-correlation data have been omitted for clarity of presentation with the exception of one typical error bar in each figure. We also note that these error bars include statistical uncertainties only.

In summary, the measured P_1 and P_2 data in Ar and Kr at 50 eV and small scattering angles were found to agree satisfactorily with theoretical predictions of first-order, perturbative theories such as the DWBA and the FOMBT. The predictions of these two theories are rather similar in the scattering regime studied here and it is difficult to judge which theory provides a better description of the measured data. The FBA, as can be expected, is incapable of describing the experimental data at all but the smallest scattering angles. The range of validity of the FBA is seen to decrease with increasing complexity of the target atom, i.e., with increasing Z.

2. *Alignment angle and linear polarization of the charge cloud*

Two natural parameters, the linear polarization P_{lin} and the alignment angle γ [cf. Eqs. (2a) and (2b)], can be extracted from the parameters P_1 and P_2. Figures 6 and 7 show the linear polarization P_{lin} and the alignment angle γ as a function of scattering angle for, respectively, Ar and Kr. In both cases, the theoretical predictions of

TABLE III. Coherence parameters P_1 and P_2 for excitation of the $5s[\frac{3}{2}]_1^0$ state in Kr at an impact energy of 50 eV and various electron-scattering angles. Given are the nominal values of P_1 and P_2 corrected for all instrumental effects where necessary (see Refs. 19, 34, and 22 for details) along with the extracted values for the alignment angle γ and the linear polarization P_{lin}. The quoted errors in P_1 and P_2 include all systematic uncertainties and one standard deviation of counting statistics.

Scattering angle (deg)	P_1	P_2	Alignment angle γ (deg)	Linear polarization P_{lin}
0±0.5	+0.98±0.14	−0.03±0.08	−0.9±2.5	0.98±0.15
5±1.5	+0.21±0.36	−0.66±0.20	−36.2±14.4	0.69±0.40
9±1.5	−0.46±0.12	−0.72±0.12	−61.3±5.5	0.85±0.17
15±1.5	−0.72±0.24	+0.35±0.22	+77.0±10.8	0.79±0.30
20±1.5	−0.18±0.15	−0.10±0.08	+14.6±19.7	0.21±0.17

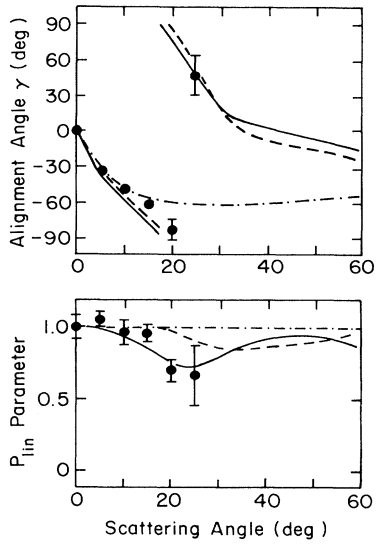

FIG. 6. Alignment angle γ and linear polarization P_{lin} for excitation of the $(^2P_{1/2})4s'[\frac{1}{2}]_{J=1}$ state in Ar at 50 eV as a function of scattering angle. The three theoretical curves represent predictions of the DWBA [24] (full line), the FOMBT [27] (dashed line), and a first Born approximation (—·—·—·). Error bars include all systematic uncertainties and one standard deviation of counting statistics. Where no error bar is indicated, the uncertainty is smaller than the plot symbol.

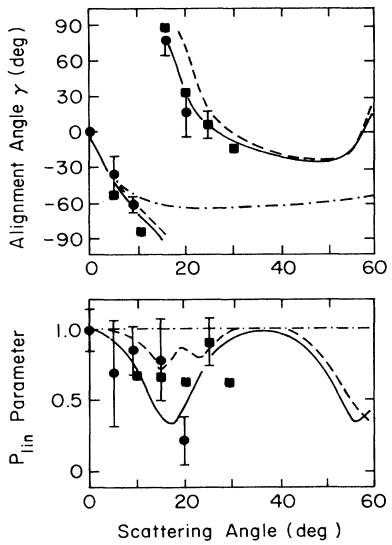

FIG. 7. Same as Fig. 6 for excitation of the $(^2P_{3/2})5s[\frac{3}{2}]_{J=1}$ state in Kr. Also shown are γ and P_{lin} values extracted from the angular correlation measurements of Danjo *et al.* (full squares) [13]. Only one typical error bar is shown for their data which represents statistical uncertainty only. The P_{lin} data point extracted from their data at 5° is outside the meaningful range of P_{lin} values from 0 to +1 and is therefore not shown.

the DWBA and the FOMBT for the alignment angle are very similar over the entire range of scattering angles studied and the measured data yield γ values which are in very good agreement with the theory. As before, the FBA starts to break down at very small scattering angles around 10°. In the case of γ, the agreement between our Kr data and the angular-correlation data of Danjo *et al.* [13] is overall satisfactory. The DWBA and the FOMBT predict a slightly different behavior of the linear polarization P_{lin} as a function of scattering angle. The deviation of P_{lin} from unity (which indicates an increased significance of angular momentum transfer perpendicular to the scattering plane) is more pronounced in the DWBA. This is consistent with our experimental findings in Ar. In Kr, on the other hand, a meaningful comparison between experiment and theory and between the two different experiments is somewhat obscured by the comparatively large error margin in both experimental data sets. We note that no P_{lin} value extracted from the angular-correlation data of Danjo *et al.* [13] is shown at 5° due to a P_2 value outside the physically meaningful range of values (see preceding section). Our Kr data seem to substantiate the drastic decline of P_{lin} around 20° which is also predicted by the DWBA. We note that the FBA mandates a value of $P_{\text{lin}}=+1$ (or $P_3=0$) independent of the scattering angle, since this theory does not account for any transfer of orbital angular momentum perpendicular to the scattering plane. Such a behavior is obviously inconsistent with either set of experimental data.

In summary, the first-order, perturbative theories seem to be quite capable of predicting the alignment angle γ of the excited-state charge cloud in the scattering plane. The differences in the predictions of the DWBA and the FOMBT were found to be too small in comparison to the accuracy of the reported experimental data to allow a meaningful distinction as to which theory agrees better with the measured data. The two theories predict a slightly different behavior of the linear polarization P_{lin}. The agreement between experiment and theory is less convincing here, indicating that it seems more difficult to calculate the exact shape of the charge cloud, i.e., the P_{lin} parameter, in the framework of first-order, perturbative theories.

V. CONCLUSIONS

We measured the linear coherence parameters P_1 and P_2 for excitation of the first excited states of the heavy noble gases Ne, Ar, and Kr in the regime of large impact parameters. Great care was exercised in identifying and quantifying the influence of those instrumental effects on the measured parameters that have recently been identified as potential sources of far-reaching systematic errors [19,21,30–34]. Our measurements of the P_1 parameter in forward scattering at impact energies from 30 to 100 eV for Ne, Ar, and Kr confirm the theoretical prediction of $P_1=+1$. This finding indicates that the excitation process is dominated by the transfer of orbital angu-

lar momentum, i.e., the direct excitation of the *LS*-coupled singlet component of the excited states. The result is also consistent with physical intuition, which suggests that exchange excitation should not play a role in the regime of very large impact parameters. Measurements of P_1 and P_2 in Kr and Ar at 50 eV and scattering angles up to 25° were found to be in satisfactory agreement with theoretical predictions of first-order, perturbative theories such as the DWBA and the FOMBT. It was also demonstrated that the FBA breaks down at comparatively large impact parameters and that the range of validity of the FBA decreases with increasing atomic number of the target. Two natural parameters, the alignment angle γ and the linear polarization P_{lin}, were extracted from the measured P_1 and P_2 values. The agreement between experiment and the predictions of the DWBA and the FOMBT was quite good in the case of γ, but less satisfactory for P_{lin}. This indicates that the theories appear to be well suited to predict the alignment angle of the angular part of the collisionally induced excited-state charge cloud in the scattering plane, but less capable of predicting the exact shape of the charge cloud. The general trend observed in the measured P_1, P_2, γ, and P_{lin} data in the case of Ar and Kr has been corroborated by very recent measurements in Ne carried out in our laboratory [48,49].

ACKNOWLEDGMENTS

We would like to thank the machine shop staff at Lehigh University (Mr. J. A. Zelinski and Mr. R. F. Wolfinger) for their technical expertise in the construction of the original coincidence apparatus. We are also grateful to the machine shop at the City College of New York (CCNY) (Mr. J. Altmann and his staff) for their assistance in modifying and improving the apparatus. The authors would like to acknowledge many helpful discussions with Dr. K. Bartschat, Dr. B. J. Stumpf, Dr. G. Csanak, Dr. J. J. Corr, Dr. G. F. Hanne, Dr. J. Kessler, Dr. M. S. Lubell, Dr. D. H. Madison, Dr. J. W. McConkey, Dr. M. H. Mittleman, Dr. S. Trajmar, Dr. P. J. M. van der Burgt, and Dr. P. W. Zetner. We are grateful to Dr. G. Csanak and Dr. G. D. Meneses for drawing our attention to the inconsistencies in the previously published FOMBT calculations for krypton and for making their latest Kr results available to us prior to publication. The material presented in this paper is based upon work supported by the National Science Foundation (NSF) through Grant Nos. PHY-8517629 (to Lehigh University), PHY-8819510 (to CCNY), and PHY-8901619 (to CCNY). We would also like to acknowledge the support of this work in its early stages by the Research Corporation through a Cottrell Research Grant.

*Present address: Jet Propulsion Laboratory, Pasadena, CA 91109

[1] M. Eminyan, K. B. MacAdam, J. A. Slevin, and H. Kleinpoppen, Phys. Rev. Lett. **31**, 576 (1973); M. Eminyan, K. B. MacAdam, J. A. Slevin, M. C. Standage, and H. Kleinpoppen, J. Phys. B **7**, 1519 (1974).

[2] K. Blum and H. Kleinpoppen, Phys. Rep. **52**, 203 (1979).

[3] J. Slevin, Rep. Prog. Phys. **47**, 461 (1984).

[4] K. Becker, H. W. Dassen, and J. W. McConkey, J. Phys. B **17**, 2535 (1984).

[5] M. A. Khakoo and J. W. McConkey, J. Phys. B **20**, 5541 (1987).

[6] N. Andersen, J. W. Gallagher, and I. V. Hertel, Phys. Rep. **165**, 1 (1988).

[7] J. A. Slevin and S. Chwirot, J. Phys. B **23**, 165 (1990).

[8] K. Blum, *Density Matrix Theory and Applications* (Plenum, New York, 1981).

[9] H. Arriola, P. J. O .Teubner, A. Ugabe, and E. Weigold, J. Phys. B **8**, 1275 (1975).

[10] A. Ugabe, P. J. O. Teubner, E. Weigold, and H. Arriola, J. Phys. B **10**, 71 (1977).

[11] A. Pochat, F. Gelebart, and J. Peresses, J. Phys. B **13**, L79 (1980).

[12] J. King, P. A. Neill, and A. Crowe, J. Phys. B **18**, L589 (1985).

[13] A. Danjo, T. Koike, K. Kani, H. Sugahara, A. Takahashi, and H. Nishimura, J. Phys. B **18**, L595 (1985).

[14] H. Nishimura, A. Danjo, and A. Takahashi, J. Phys. B **19**, L167 (1986).

[15] K. D. Murray, S. F. Gough, P. A. Neill, and A. Crowe, J. Phys. B **23**, 2137 (1990).

[16] I. C. Malcolm and J. W. McConkey, J. Phys. B **12**, 511 (1979).

[17] M. A. Khakoo and J. W. McConkey, Phys. Rev. Lett. **57**, 679 (1986).

[18] P. Plessis, M. A. Khakoo, P. Hammond, and J. W. McConkey, J. Phys. B **21**, L483 (1988).

[19] K. E. Martus and K. Becker, J. Phys. B **22**, L497 (1989).

[20] K. E. Martus and K. Becker, in *Proceedings of the 16th International Conference on the Physics of Electronic and Atomic Collisions, New York, 1989,* edited by A. Dalgarno, R. S. Freund, M. S. Lubell, and T. B. Lucatorto (AIP, New York, 1989), p. 169; K. E. Martus, S. H. Zheng, and K. Becker, in *Proceedings of the VIIth International Conference on Atomic Physics, Ann Arbor (1990),* edited by W. E. Baylis, J. W. McConkey, and G. W. F. Drake (University of Windsor Press, Windsor, 1990), p. VI-2.

[21] J. J. Corr, P. J. M. van der Burgt, P. Plessis, M. A. Khakoo, P. Hammond, and J. W. McConkey, J. Phys. B **24**, 1069 (1990).

[22] J. J. Corr, P. Plessis, and J. W. McConkey, Phys. Rev. A **42**, 5240 (1990).

[23] V. V. Balashov, I. V. Kozhevnikov, and A. I. Magunov, J. Phys. B **14**, 2059 (1981).

[24] K. Bartschat and D. H. Madison, J. Phys. B **20**, 5839 (1987).

[25] L. E. Machado, E. P. Leal, and G. Csanak, J. Phys. B **15**, 1773 (1982).

[26] L. E. Machado, E. P. Leal, and G. Csanak, Phys. Rev. A **29**, 1811 (1984).

[27] F. J. da Paixao, N. T. Padial, and G. Csanak, Phys. Rev. A **30**, 1697 (1984).

[28] G. D. Meneses, F. J. da Paixao, and N. T. Padial, Phys. Rev. A **32**, 156 (1985).

[29] G. Csanak and G. Meneses (private communication); it has been brought to the authors' attention that there are inconsistencies in the previous calculations for krypton (Ref. [26]). An improved set of FOMBT coherence pa-

rameters has been calculated just recently and is planned to be published shortly.
[30] P. W. Zetner, S. Trajmar, G. Csanak, and R. E. H. Clark, Phys. Rev. A **39**, 6022 (1989).
[31] P. W. Zetner, S. Trajmar, and G. Csanak, Phys. Rev. A **41**, 5980 (1990).
[32] T. Simon, M. Sohn, G. F. Hanne, and K. Bartschat, J. Phys. B **23**, L259 (1990).
[33] P. J. M. van der Burgt, J. J. Corr, and J. W. McConkey, J. Phys. B **24**, 1049 (1990).
[34] K. E. Martus, K. Becker, and D. H. Madison, Phys. Rev. A **38**, 4876 (1988).
[35] K. Rubin, B. Bederson, M. Goldstein, and R. E. Collins, Phys. Rev. **282**, 182 (1969).
[36] J. Wykes, J. Phys. B **5**, 1126 (1972).
[37] J. Macek and D. H. Jaecks, Phys. Rev. A **4**, 2288 (1971).
[38] U. Fano and J. H. Macek, Rev. Mod. Phys. **45**, 553 (1973).
[39] D. F. Register, S. Trajmar, G. Csanak, S. W. Jensen, M. A. Fineman, and R. T. Poe, Phys. Rev. A **28**, 151 (1983).
[40] Leybold Heraeus, Vacuum Technology and Reference Data Handbook.
[41] J. N. H. Brunt, G. C. King, and F. H. Read, J. Phys. B **18**, 3781 (1977).
[42] W. B. Westerveld, K. Becker, P. W. Zetner, J. J. Corr, and J. W. McConkey, Appl. Opt. **24**, 2256 (1985).
[43] D. W. Lynch and W. R. Hunter, in *Handbook of Optical Constants of Solids,* edited by E. D. Palik (Academic, New York, 1985), p. 286.
[44] P. Hammond, W. Karras, A. G. McConkey, and J. W. McConkey, Phys. Rev. A **40**, 1804 (1989).
[45] G. Csanak and D. C. Cartwright, J. Phys. B **22**, 2769 (1989).
[46] G. F. Hanne, Phys. Rep. **95**, 97 (1983).
[47] G. F. Hanne, in *Coherence in Atomic Collision Processes,* edited by H. J. Beyer *et al.* (Plenum, New York, 1988), p. 41.
[48] K. E. Martus, S. H. Zheng, and K. Becker, Bull. Am. Phys. Soc. (to be published).
[49] K. Becker, J. W. McConkey, and A. Crowe, J. Phys. B (to be published).